

Research Article

Change in the Pathologic Supraspinatus: A Three-Dimensional Model of Fiber Bundle Architecture within Anterior and Posterior Regions

Soo Y. Kim,¹ Rohit Sachdeva,¹ Zi Li,² Dongwoon Lee,³ and Benjamin W. C. Rosser⁴

¹School of Physical Therapy, College of Medicine, University of Saskatchewan, Saskatoon, SK, Canada S7N 0W3

²Department of Surgery, University of Toronto, Toronto, ON, Canada M5T 1P5

³Department of Computer Science, University of Toronto, Toronto, ON, Canada M5S 3G4

⁴Department of Anatomy and Cell Biology, College of Medicine, University of Saskatchewan, Saskatoon, SK, Canada S7N 5E5

Correspondence should be addressed to Soo Y. Kim; soo.kim@usask.ca

Received 18 February 2015; Revised 2 April 2015; Accepted 3 April 2015

Academic Editor: Heather F. Smith

Copyright © 2015 Soo Y. Kim et al. This is an open access article distributed under the Creative Commons Attribution License, which permits unrestricted use, distribution, and reproduction in any medium, provided the original work is properly cited.

Supraspinatus tendon tears are common and lead to changes in the muscle architecture. To date, these changes have not been investigated for the distinct regions and parts of the pathologic supraspinatus. The purpose of this study was to create a novel three-dimensional (3D) model of the muscle architecture throughout the supraspinatus and to compare the architecture between muscle regions and parts in relation to tear severity. Twelve cadaveric specimens with varying degrees of tendon tears were used. Three-dimensional coordinates of fiber bundles were collected *in situ* using serial dissection and digitization. Data were reconstructed and modeled in 3D using Maya. Fiber bundle length (FBL) and pennation angle (PA) were computed and analyzed. FBL was significantly shorter in specimens with large retracted tears compared to smaller tears, with the deeper fibers being significantly shorter than other parts in the anterior region. PA was significantly greater in specimens with large retracted tears, with the superficial fibers often demonstrating the largest PA. The posterior region was absent in two specimens with extensive tears. Architectural changes associated with tendon tears affect the regions and varying depths of supraspinatus differently. The results provide important insights on residual function of the pathologic muscle, and the 3D model includes detailed data that can be used in future modeling studies.

1. Introduction

Supraspinatus tendon tears of the rotator cuff are associated with changes in both the tendon and muscle. Fraying and thinning of the lateral aspect of the tendon occur with full-thickness tears [1, 2]. Muscular inhibition and disuse due to pain can lead to changes in the muscle. A decrease in muscle volume and fat infiltration can occur with large tendon tears [3–5]. The musculotendinous unit of the supraspinatus can also retract medially altering the length of fiber bundles [6, 7]. The alignment of fiber bundles relative to the axis of pull or line of force which is known as the pennation angle (PA) can also change as a result of retraction [8].

The function of a muscle is directly correlated with its architecture. Among the architectural parameters of skeletal muscles, fiber bundle length (FBL) is known to be the most

important as it is proportional to muscle excursion and the velocity of contraction [9, 10]. A direct linear relationship has been found between muscle length and force of isometric contraction [11]. Thus, a change in FBL can affect the optimal range and speed at which a muscle contracts [12]. In pennated muscles, only a component of the muscle fibers' force is projected onto the line of force; thus a change in PA will also impact the force-producing capabilities [13].

The muscle and tendon architecture of the supraspinatus is complex. The normal muscle has two main regions, anterior and posterior [14–18], which have been found to be functionally distinct [19–21]. The anterior region accounts for 75–86% of the muscle volume and its pennated fiber bundles attach laterally to the anterior tendon [14, 16]. It produces the majority of force for the muscle [14, 16]. The posterior region is substantially smaller in volume and partially lies

deep to the anterior. The parallel fiber bundles attach laterally to the posterior tendon [14, 16]. Based on its architecture, dynamic FBL changes with shoulder movements [19], fiber type composition [20], and innervation pattern [21], the posterior region is thought to play an important role in adjusting tension on the rotator cuff. Within each region there are three distinct parts, superficial, middle, and deep, based on the lateral attachment sites onto the tendon and fiber bundle orientation [16].

To date, the fiber bundle architecture of the pathologic supraspinatus has not been investigated throughout the muscle volume. In previous investigations, fiber bundle measurements were taken from the superficial surface of the muscle, not accounting for the different regions and parts of the muscle [6, 7]. Since the length of fiber bundles and PA are directly related to skeletal muscle function [22], it is important to quantify these parameters for both the anterior and posterior regions of the pathologic supraspinatus. In addition, given that architectural changes are considered to be the most important pathophysiological consequence of tendon tears and a critical factor in the success of tendon repair surgery, a thorough understanding of these parameters is needed [23].

A robust fiber bundle architecture database of the pathologic supraspinatus can be used to advance three-dimensional (3D) musculoskeletal computer models of the shoulder. 3D modeling is a powerful tool for analyzing the biomechanics underlying normal and pathological movements, particularly in complex systems such as the shoulder [24, 25]. Finite-element muscle models can provide detailed information about the distribution of strain within a muscle and the transmission of force [24]. These models, which are dependent on accurate fiber bundle data, can be used to make clinically relevant predictions about the functional deficits caused by rotator cuff tendon tears and the functional outcomes following surgery and rehabilitation [26, 27].

The purpose of this study was to investigate and model the muscle architecture throughout the volume of the supraspinatus using cadaveric specimens with varying degrees of tendon tears. It was hypothesized that fiber bundle architecture would differ between the anterior and posterior regions and their respective parts, superficial, middle, and deep, and that the architectural changes would be associated with the degree of tendon pathology.

2. Materials and Methods

2.1. Specimens. Twelve formalin embalmed cadaveric shoulder specimens (3 males, 9 females) with evidence of supraspinatus tendon pathology, that is, partial thickness or full-thickness tears, were used. Mean age was 82.1 ± 10.8 years with a range of 64–95. Ethics approval was obtained from the Biomedical Research Ethics Board, University of Saskatchewan (Bio#11-77).

To expose the muscle and determine the presence of supraspinatus tendon pathology all overlying soft tissues (skin, fascia, trapezius, and deltoid) were removed. The clavicle and lateral aspect of the acromion were also removed to

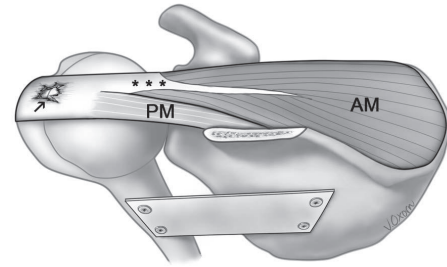


FIGURE 1: Supraspinatus with full-thickness tendon tear with no retraction (specimen representative of category B). Superior view of the middle part of the muscle belly with acromion removed. Fiber bundles of the superficial parts of anterior and posterior regions have been removed. Specimen stabilized with metal plate. Anterior part of supraspinatus tendon represented by ***; middle part of anterior region (AM); middle part of posterior region (PM). Fiber bundles of deep parts lie deep to the AM and PM. Arrow (↑) points to a full-thickness tear illustrated on the supraspinatus tendon.

allow full visualization of the rotator cuff tendons. Specimens with evidence of shoulder surgery or gross bony deformities were not used.

Specimens were placed into one of three categories based on the degree of tendon tear of the supraspinatus: (A) partial thickness tear; (B) full-thickness tear with no tendon retraction; (C) full-thickness tear with tendon retraction. A tear was deemed as having tendon retraction when the tear involved the entire extent (width) of the supraspinatus tendon in the sagittal plane. In specimens with full-thickness tendon tears (“B” and “C”), coronal and sagittal dimensions of the tear were measured using a digital caliper (Traceable ISO 17025 Calibrated, Fisher Scientific, Nepean, ON, Canada) and recorded.

2.2. Dissection and Digitization. Each of the 12 specimens was digitized. Previously developed digitization protocols for human skeletal muscles were adapted for this study [16, 28]. The glenohumeral joint was stabilized in 0° of abduction, flexion, and lateral rotation with a metal plate screwed to the humerus and scapula (Figure 1). The lateral aspect of the scapular spine, coracoid process, and greater tubercle were selected as reference points and demarcated with screws. These reference points were used in the modeling process and assisted in reconstructing the specimen in 3D. Specimens were then clamped into a securely mounted vice.

The periphery of the supraspinatus tendon was outlined with small dots 2 mm apart using a paint pen. Next, each point was digitized using a Microscribe G2X Digitizer (Immersion Corporation, San Jose, CA, USA). Following this, the division between the anterior and posterior regions on the superficial surface of the muscle as defined by Kim et al. [16] was identified and marked with small pins (3 mm in length). The anterior region of the supraspinatus muscle belly was serially dissected and digitized *in situ* first. Starting with the most superficial layer, 10–60 fiber bundles were identified. Each fiber bundle was then digitized using 10–20 sequential sites, beginning at the medial attachment site and ending at

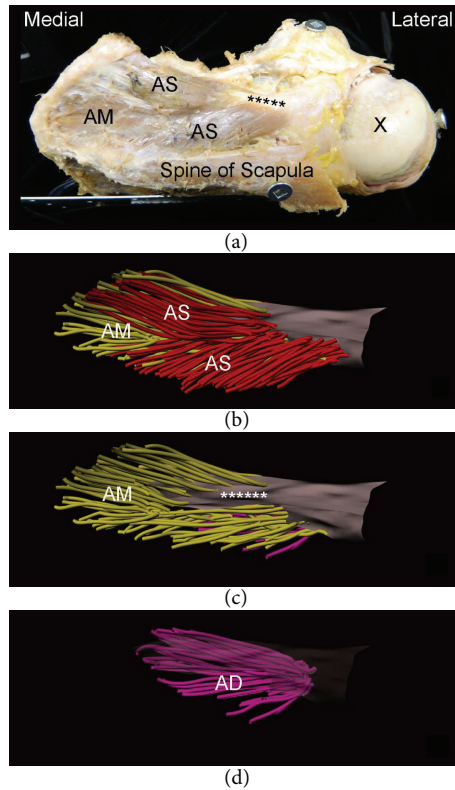


FIGURE 2: Retracted full-thickness tendon tear of supraspinatus without a distinguishable posterior region modelled throughout its volume in 3D (specimen from category C). (a) Superior view of specimen with lateral aspect of spine of scapula removed; superficial part of anterior region (AS); middle part of anterior region (AM); * * * intramuscular portion of anterior supraspinatus tendon. Metal plate (bottom left) was used to stabilize the specimen and screws (scapular spine, coracoid process, and greater tubercle) were used in modeling process. (b) Computer model of anterior region including AS (red fibers) and AM (yellow fibers). (c) AM; AS not shown; (d) deep part of anterior region (AD) (pink fibers); AS, AM, and tendon are not shown.

the lateral. Once the entire layer had been digitized, fiber bundles were carefully removed to expose the underlying fascicles about 1-2 mm deeper. The periphery of the tendon was digitized whenever the tendon shape was found to change which was approximately at every 3–5 mm of the muscle’s depth. Once the entire anterior region had been digitized, the posterior region was serially dissected and digitized as outlined above.

2.3. *Modeling.* Digitized data were exported to Autodesk Maya 2009 (Autodesk, San Jose, CA, USA) and reconstructed in 3D using plug-ins developed in the laboratory. Fiber bundles and their attachment onto the tendon could be clearly visualized volumetrically using the model. Architecturally distinct regions and parts as defined by Kim et al. [16] were identified and color coded (Figure 2).

2.4. *Data Analysis.* Fiber bundle lengths and PA were computed with algorithms used in previously published work [16, 29, 30]. For a detailed description of computational methods the reader is referred to Lee et al. [29, 30]. Digitized fiber bundles were first reconstructed into an interpolating

cubic Catmull-Rom spline. Using arc-length parameterisation, digitized points were then resampled to make the curve representation uniform. FBL was approximated as an entire arc-length of the curve [29]. In the present study, PA is defined as an angle between the fiber bundle orientation and the line of force. The fiber bundle orientation was estimated by a tangent vector along the curve. The tangent vectors at the lateral and medial attachment sites were calculated as average derivatives of the curve over the lateral and medial regions, respectively [29, 30]. Hence, two angles were computed, lateral PA and medial PA. The line of force was determined as a vector best approximating the axis of the intramuscular tendon.

Statistical analysis was carried out using SPSS (version 18.0, Chicago, IL, USA). All architectural parameters for the anterior and posterior regions and their distinct parts were characterized with descriptive statistics (median and minimum-maximum values). Mann-Whitney *U* tests were used to compare median tear dimensions between specimen categories B and C and architectural parameters between categories of A and B of the posterior region. The Kruskal-Wallis test followed by pairwise comparisons (Mann-Whitney *U* tests) was used to compare median age of specimens and

TABLE 1: Summary of specimens.

Specimen #	Side	Sex	Age	Tear category	RCT location	Coronal plane (cm)	Sagittal plane (cm)
1460	R	F	67	A	SP	—	—
1463	R	F	95	A	SP	—	—
1429	R	F	64	A	SP	—	—
1425	R	M	89	A	SP	—	—
1458	R	F	73	B	SP	1.88	1.63
1450	R	F	77	B	SP	1.04	2.08
1447	R	F	94	B	SP	1.47	1.52
1447	L	F	94	B	SP	1.40	1.17
1455*	R	F	82	C	SP, SSC, ISP	3.33	3.84
1427*	R	M	76	C	SP, SSC, ISP	5.0	3.00
1444	R	M	83	C	SP, SSC, ISP	2.59	3.76
1445	L	F	91	C	SP, SSC, ISP	2.59	3.67

*Specimens with no posterior region. R: right; L: left; F: female; M: male; RCT: rotator cuff tear; A: partial thickness tear; B: full-thickness tear with no retraction; C: full-thickness tear with retraction of the tendon; SP: supraspinatus; SCC: subscapularis; ISP: infraspinatus; —: not measured.

architectural parameters between the three tear categories and between superficial, middle, and deep parts. Significance was accepted at $P < 0.05$ with Bonferroni adjustments made where appropriate ($0.05/3 = 0.0167$).

3. Results

3.1. Tendon Morphology. Within each of the three tendon tear categories, there were four specimens. The largest diameters of the tear in the coronal and sagittal planes, measured in specimens of categories B and C, are presented in Table 1. The median tear dimensions in category C (2.96 cm for coronal plane; 3.72 cm for sagittal plane) were significantly larger than those in category B (1.58 cm for coronal plane; 1.44 cm for sagittal plane) for both planes ($P = 0.020$ for coronal and $P = 0.021$ for sagittal). All specimens in category C also had a tear of the infraspinatus and subscapularis tendons. There was no difference in the median age of specimens between categories.

3.2. Muscle Morphology

3.2.1. Anterior Region. Table 2 provides a summary of the architectural parameters of the anterior region as a whole. In all specimens an anterior region was present (Figure 1). Median FBL significantly differed between the three tear categories ($P < 0.001$). Specimens of category C had the shortest fibers. Median lateral PA in category C was significantly larger than categories A and B ($P < 0.001$). Median medial PA significantly differed between all tear categories ($P < 0.001$), with the largest PA found in category C.

Table 3 provides a summary of median FBL values of the superficial, middle, and deep parts within the anterior region. Median FBL was significantly different between all the parts in each tear category. The significance level was $P < 0.001$ except between the superficial and deep in category B and the middle and deep in category C, which was $P = 0.001$.

The middle and deep parts were shorter than the superficial in all categories.

Tables 4 and 5 provide a summary of median lateral and medial PA values of the superficial, middle, and deep parts within the anterior region. Median lateral PA of the superficial part was significantly larger than the middle ($P < 0.001$) in category B. No statistical difference was found between the superficial and deep ($P = 0.022$) and middle and deep ($P = 0.071$). No statistical difference was found between parts in category A ($P = 0.167$) or category C ($P = 0.274$). Median medial PA of the superficial part was significantly larger than the middle and deep ($P < 0.001$) in all tear categories. No statistical difference was found between the middle and deep ($P = 0.163$) in category A. In categories B and C, median medial PA was significantly different between all parts ($P < 0.001$).

3.2.2. Posterior Region. Architectural parameters for the posterior region as a whole are summarized in Table 2. In two specimens of category C a distinct posterior region was absent (Figure 2). Due to the reduced sample size in category C, statistical analysis of these specimens was not carried out. Median FBL significantly differed between categories A and B ($P < 0.001$). Median lateral PA significantly differed between categories A and B ($P = 0.013$). Median lateral PA in category A was larger than category B ($P = 0.013$). Median medial PA in category A was significantly larger than that of category B ($P < 0.001$).

Median FBL values for the superficial, middle, and deep parts within the posterior region are summarized in Table 3. In category A, median FBL of the middle part was significantly longer than that of the superficial and deep ($P < 0.001$). No statistical difference was found between the superficial and deep ($P = 0.699$). In category B, no difference was found between parts ($P = 0.114$).

A summary of median lateral and medial PAs of the superficial, middle, and deep parts within the posterior region can be found in Tables 4 and 5. Median lateral PA

TABLE 2: Median values of architectural parameters for anterior and posterior regions.

Region of muscle and tear category	<i>n</i>	FBL (cm)	PA lat. (degree)	PA med. (degree)
Anterior				
A	4	6.76 ^a (3.21–10.26)	14.95 ^{a*} (2.04–45.24)	13.81 ^a (2.17–45.11)
B	4	4.97 ^b (2.59–9.86)	13.91 ^{a*} (2.01–46.37)	14.77 ^b (2.02–46.63)
C	4	2.65 ^c (0.54–8.98)	23.02 ^b (2.06–80.38)	24.34 ^c (2.01–89.20)
Posterior				
A	4	5.89 ^a (2.12–8.52)	24.14 ^{a***} (2.04–38.81)	15.94 ^a (3.78–34.52)
B	4	4.81 ^b (1.48–8.92)	20.61 ^{b***} (4.42–47.55)	11.98 ^b (2.10–34.68)
C	2	3.02 [†] (1.59–4.76)	31.95 [†] (2.42–55.23)	14.29 [†] (4.83–33.15)

A: partial thickness tendon tear; B: full-thickness tear with no retraction of tendon; C: full-thickness tendon tear with retraction; FBL: fiber bundle length; PA lat.: lateral pennation angle; PA med.: medial pennation angle; () minimum and maximum values. If superscript letters are different, it indicates statistically significant difference of $P < 0.001$ of parameter between tear categories within the same region. * $P = 0.100$; ** $P = 0.013$; † statistical analysis was not conducted due to sample size.

TABLE 3: Median FBL values for the superficial, middle, and deep parts of the anterior and posterior regions.

Region of muscle and tear category	<i>n</i>	FBL (cm)		
		Superficial	Middle	Deep
Anterior				
A	4	7.56 ^a (5.36–10.26)	6.71 ^b (3.21–10.01)	6.24 ^c (3.38–8.68)
B	4	5.58 ^{a*} (2.97–9.68)	4.71 ^b (2.59–9.86)	5.16 ^{c*} (2.70–9.05)
C	4	2.95 ^a (1.45–8.98)	2.57 ^{b*} (1.04–7.19)	2.50 ^{c*} (0.54–5.41)
Posterior				
A	4	5.89 ^{a***} (2.12–8.47)	6.42 ^b (2.79–7.91)	5.85 ^{a***} (3.19–8.52)
B	4	4.88 ^{a***} (2.13–7.82)	4.98 ^{a***} (1.50–8.92)	4.65 ^{a***} (1.48–8.54)
C	2	2.96 [†] (1.90–4.47)	3.48 [†] (1.93–4.76)	2.80 [†] (1.59–4.59)

A: partial thickness tendon tear; B: full-thickness tear with no retraction of tendon; C: full-thickness tendon tear with retraction; FBL: fiber bundle length; median with () minimum and maximum values. If superscript letters are different, it indicates statistically significant ($P < 0.001$) difference between the superficial, middle, and deep parts of specimens within the same tear category. * $P = 0.001$; ** $P = 0.699$; *** $P = 0.114$; † statistical analysis was not conducted due to sample size.

TABLE 4: Median lateral PA values for the superficial, middle, and deep parts of the anterior and posterior regions.

Region of muscle and tear category	<i>n</i>	PA lat. (degree)		
		Superficial	Middle	Deep
Anterior				
A	4	14.26 ^{a*} (2.62–45.24)	15.71 ^{a*} (2.04–40.86)	14.15 ^{a*} (2.37–35.39)
B	4	15.59 ^{a***} (2.27–46.37)	12.73 ^{b***} (2.01–42.70)	14.15 ^{ab***} (2.89–40.38)
C	4	25.16 ^{a****} (2.06–64.58)	22.92 ^{a****} (2.18–80.38)	21.80 ^{a****} (3.15–74.67)
Posterior				
A	4	26.39 ^{a****} (2.04–38.81)	25.60 ^{a****} (2.19–36.34)	18.79 ^b (3.92–36.57)
B	4	27.17 ^a (9.86–41.02)	23.43 ^b (4.42–47.55)	17.71 ^c (6.32–32.00)
C	2	38.46 [†] (7.82–55.23)	35.25 [†] (2.42–51.13)	25.17 [†] (2.55–46.18)

A: partial thickness tendon tear; B: full-thickness tear with no retraction of tendon; C: full-thickness tendon tear with retraction; PA lat.: lateral pennation angle; median with () minimum and maximum values. If superscript letters are different, it indicates statistically significant ($P < 0.001$) difference between the superficial, middle, and deep parts of specimens within the same tear category. * $P = 0.167$; ** $P = 0.022$ superficial and deep, $P = 0.071$ middle and deep; *** $P = 0.274$; **** $P = 0.238$; † statistical analysis was not conducted due to sample size.

of the superficial and middle parts was significantly larger than the deep ($P < 0.001$) in category A. No statistical difference was found between the superficial and middle ($P = 0.238$). In category B, median lateral PA significantly differed between all parts ($P < 0.001$) with the largest being

in the superficial part. Median medial PA of the superficial part was significantly larger than the middle ($P < 0.001$) in category A. No statistical difference was found between the deep and middle ($P = 0.021$) or superficial ($P = 0.026$). In category B, median medial PA of the superficial part was

TABLE 5: Median medial PA values for the superficial, middle, and deep parts of the anterior and posterior regions.

Region of muscle and tear category	n	PA med. (degree)		
		Superficial	Middle	Deep
Anterior				
A	4	15.58 ^a (2.19–29.78)	12.97 ^b (2.20–45.11)	13.87 ^{b*} (2.17–30.51)
B	4	19.22 ^a (3.88–44.64)	15.95 ^b (2.02–46.63)	11.52 ^c (2.34–27.95)
C	4	28.40 ^a (2.37–89.20)	22.96 ^b (2.01–85.95)	19.99 ^c (2.17–89.11)
Posterior				
A	4	17.85 ^a (7.14–34.52)	14.46 ^{b***} (4.52–31.42)	16.54 ^{ab***} (3.78–32.19)
B	4	14.06 ^{a***} (2.96–34.68)	13.55 ^{ab***} (2.10–23.96)	10.71 ^{b***} (2.20–33.36)
C	2	19.40 [†] (4.83–33.15)	12.58 [†] (5.29–23.38)	13.89 [†] (5.39–26.37)

A: partial thickness tendon tear; B: full-thickness tear with no retraction of tendon; C: full-thickness tendon tear with retraction; PA med.: medial pennation angle; median with () minimum and maximum values. If superscript letters are different, it indicates statistically significant ($P < 0.001$) difference between the superficial, middle, and deep parts of specimens within the same tear category. * $P = 0.163$ middle and deep; ** $P = 0.026$ superficial and deep, $P = 0.021$ middle and deep; *** $P = 0.047$ superficial and middle, $P = 0.002$ superficial and deep, and $P = 0.419$ middle and deep; $P = 0.208$ middle and deep. [†]Statistical analysis was not conducted due to sample size.

significantly larger than that of the deep ($P = 0.002$). No statistical difference was found between the middle and deep ($P = 0.419$) or superficial ($P = 0.047$).

4. Discussion

This is the first study to investigate and model the fiber bundle architecture of the pathologic supraspinatus throughout the muscle volume including the anterior and posterior regions and their respective parts. We demonstrate that significant changes in architecture occur with rotator cuff tendon pathology and these changes are not uniform for the anterior and posterior regions of supraspinatus.

Median FBL of the anterior and posterior regions significantly differed between the tear categories, with a gradual decrease in FBL occurring as the size of the tear increased. Significant shortening of FBL with tendon tears has been reported in two previous studies [6, 7]. In both studies, however, only the anterior region was investigated as per reported lateral attachment of fiber bundles onto the intramuscular tendon. In addition, length measurements were taken from just two to three fibers from superficial surface of the anterior region of each specimen. Based on our model, we know that both anterior and posterior regions undergo significant shortening with tendon tears. Shortening of muscle fibers and tendon retraction are barriers for structural healing following open and arthroscopic tendon repair [31]. When structural healing is not achieved, recovery of strength has been poorer and the glenohumeral joint may be more prone to degenerative changes [31, 32].

In the normal supraspinatus, FBLs within the superficial, middle, and deep parts of the anterior region were found to be uniform [16]. In the present study of the pathologic muscle, however, in general as the severity of the tear increased a progressive shortening of FBLs from the superficial to deep parts was observed. This pattern of FBL change within the volume of the anterior region could be of clinical importance. First, tears on the articular surface of the supraspinatus

tendon are two to three times more frequent than bursal-sided tears [33, 34]. Our findings further support this prevalence and suggest tears involving the anterior portion of the supraspinatus tendon propagate from the articular surface toward the bursal surface. Secondly, as a consequence of this progressive shortening starting in the deep part of the muscle, the deeper fibers may undergo greater stretching during tendon repair. To achieve tendon to bone repair, the torn and often retracted musculotendinous unit is mobilized laterally. Overstretching, particularly of the shortened deep fibers, can cause damage and lead to proliferation of non-contractile tissue [33]. Furthermore, the articular side of the supraspinatus tendon has been found to experience more strain compared to the bursal surface under uniaxial loading [35]. These tendon strain patterns may be correlated with the pattern of FBL changes observed in this study.

In the posterior region, the pattern of progressive shortening of FBLs from the superficial to deep parts was not observed. The differences found between the anterior and posterior regions may be related in part to the differences in muscle architecture. For example, the fibers of the anterior region are in a penniform configuration, while in the posterior region they are fusiform.

A decrease in FBL will decrease the absolute active muscle range and maximum contraction velocity [36]. In the torn supraspinatus, sarcomeres have been found to maintain their optimal operating length [7]. Tomioka et al. [7] found no significant difference in sarcomere length of the supraspinatus between the intact and torn tendon specimens examined. Despite this maintenance, a recent study investigating the contractility of muscle fibers sampled from patients with chronic full-thickness tears found a 30% reduction in the maximum isometric force production [37]. The normalized force production was found to be negatively correlated with tear size [37]. The architectural changes documented in our study will compound these force production deficits reported by Mendias et al. [37]. Our data on FBL along with insights of sarcomere lengths changes [7] and muscle fiber contractility [37] can be used in future computer modeling studies to

predict the changes in active range and contraction velocity of the pathologic muscle and to simulate the biomechanical effects on the shoulder complex.

An increase in PA with rotator cuff tendon tears has been previously reported with larger and retracted tears being correlated with larger angles [8, 17]. Although direct comparison of our PA values with those from other cadaveric and imaging studies is difficult due to differences in measurement methods, our findings support the general trends reported in these previous studies. In the present study, median lateral and medial PAs of the anterior region were significantly larger in specimens with a retracted tendon. In contrast, the median lateral and medial PAs of the posterior region were significantly larger in specimens with partial tears compared to full-thickness tears. Again, these regional differences may be attributed to differences in muscle architecture and possibly the location of the tendon pathology, that is, articular versus bursal sided and/or anterior versus posterior.

The posterior region of the supraspinatus was present in all normal specimens examined by Kim et al. [16] and Roh et al. [14]. The absence of a distinguishable posterior region in half of the specimens with large retracted tendon tears in the present study raises important clinical questions given the broad lateral attachment of fibers onto the supraspinatus tendon and its distinct function [18–21]. First, what is the functional impact of not having a posterior region in both the unrepaired and repaired tendon states? Since the posterior region is thought to quickly adjust tension on the rotator cuff, preventing buckling of the tendon with dynamic movement [20, 21], the loss of this region can have a significant functional impact. The residual function of the pathological muscle thus needs to be better understood. Expectations and approaches for rehabilitation and surgical repair may also need to be altered when there is loss of the posterior region. Secondly, is loss of the posterior region an eventual change that occurs with chronic tendon tears? It is known that chronicity of the tendon tear is positively related to rotator cuff muscle atrophy [38, 39]. As the volume of the posterior region is significantly smaller than that of the anterior region in the normal muscle [14, 16] even a small amount of atrophy could considerably impact the posterior region. If atrophy or complete loss is indeed found to be an eventual consequence of chronic tears, it would further underscore the importance of early detection of the tear and repair of the tendon. Delayed detection of tears is associated with surgical complications and inferior outcomes [40] and extensive changes to the posterior region may play a role in these problems.

5. Conclusions

The fiber bundle architecture of both anterior and posterior regions was investigated and distinct patterns of change were found. Fiber bundle length shortening is associated with the degree of tendon tear with the fibers of the deep part showing the greatest degree of shortening. Pennation angle changes are also related to the degree of tendon tear, with the superficial fibers possibly undergoing greater changes than other parts of the muscle. The posterior region

was completely absent in specimens with extensive tendon tears raising several clinically relevant questions that need to be further explored. Since the supraspinatus muscle is an important dynamic stabilizer of the glenohumeral joint and most commonly involved with rotator cuff pathology, a thorough understanding of the muscle changes is essential. It is expected that the model created in this study will be used to advance computer models that can simulate different surgical techniques and rehabilitation protocols. Furthermore, the model can be incorporated with existing shoulder models to be used for biomechanical analysis in different patient populations with supraspinatus tendon pathologies.

Conflict of Interests

The authors declare that there is no conflict of interests regarding the publication of this paper.

Acknowledgments

The authors would like to acknowledge the Saskatchewan Health Research Foundation (SHRF) for funding this project. They would like to express gratitude to the families who participated in the Body Bequeathal Program of the Department of Anatomy and Cell Biology, College of Medicine, University of Saskatchewan. They also thank Corrie Willfong and David Shewchuk, technical staff of the Department of Anatomy and Cell Biology, Autodesk Inc., for providing the research/educational license for Autodesk Maya 2009 (Autodesk Inc., San Rafael, CA, USA), Valerie Oxorn, B.A., M.A., M.S., B.M.C., Medical Illustrator, for illustrating Figure 1, and the College of Medicine, University of Saskatchewan.

References

- [1] C. J. Petersson, "Ruptures of the supraspinatus tendon. Cadaver dissection," *Acta Orthopaedica Scandinavica*, vol. 55, no. 1, pp. 52–56, 1984.
- [2] X. Liu, D. Laron, K. Natsuhara, G. Manzano, H. T. Kim, and B. T. Feeley, "A mouse model of massive rotator cuff tears," *The Journal of Bone & Joint Surgery—American Volume*, vol. 94, no. 7, article e41, 2012.
- [3] D. Goutallier, J.-M. Postel, J. Bernageau, L. Lavau, and M.-C. Voisin, "Fatty muscle degeneration in cuff ruptures: pre- and postoperative evaluation by CT scan," *Clinical Orthopaedics and Related Research*, no. 304, pp. 78–83, 1994.
- [4] D. Goutallier, J.-M. Postel, P. Gleyze, P. Leguilloux, and S. Van Driessche, "Influence of cuff muscle fatty degeneration on anatomic and functional outcomes after simple suture of full-thickness tears," *Journal of Shoulder and Elbow Surgery*, vol. 12, no. 6, pp. 550–554, 2003.
- [5] C. Gerber, D. C. Meyer, E. Frey et al., "Neer Award 2007: reversion of structural muscle changes caused by chronic rotator cuff tears using continuous musculotendinous traction. An experimental study in sheep," *Journal of Shoulder and Elbow Surgery*, vol. 18, no. 2, pp. 163–171, 2009.
- [6] E. Itoi, H.-C. Hsu, S. W. Carmichael, B. F. Morrey, and K.-N. An, "Morphology of the torn rotator cuff," *Journal of Anatomy*, vol. 186, no. 2, pp. 429–434, 1995.

- [7] T. Tomioka, H. Minagawa, H. Kijima et al., "Sarcomere length of torn rotator cuff muscle," *Journal of Shoulder and Elbow Surgery*, vol. 18, no. 6, pp. 955–959, 2009.
- [8] J. Zuo, H. Sano, and E. Itoi, "Changes in pennation angle in rotator cuff muscles with torn tendons," *Journal of Orthopaedic Science*, vol. 17, no. 1, pp. 58–63, 2012.
- [9] R. L. Lieber and S. R. Ward, "Skeletal muscle design to meet functional demands," *Philosophical Transactions of the Royal Society B: Biological Sciences*, vol. 366, no. 1570, pp. 1466–1476, 2011.
- [10] R. L. Lieber and J. Fridén, "Clinical significance of skeletal muscle architecture," *Clinical Orthopaedics and Related Research*, no. 383, pp. 140–151, 2001.
- [11] J. B. Morrison, "The mechanics of muscle function in locomotion," *Journal of Biomechanics*, vol. 3, no. 4, pp. 431–451, 1970.
- [12] R. L. Lieber and S. C. Bodine-Fowler, "Skeletal muscle mechanics: implications for rehabilitation," *Physical Therapy*, vol. 73, no. 12, pp. 844–856, 1993.
- [13] C. Gans and A. S. Gaunt, "Muscle architecture in relation to function," *Journal of Biomechanics*, vol. 24, no. 1, pp. 53–65, 1991.
- [14] M. S. Roh, V. M. Wang, E. W. April, R. G. Pollock, L. U. Bigliani, and E. L. Flatow, "Anterior and posterior musculotendinous anatomy of the supraspinatus," *Journal of Shoulder and Elbow Surgery*, vol. 9, no. 5, pp. 436–440, 2000.
- [15] A. D. Ward, G. Hamarneh, R. Ashry, and M. E. Schweitzer, "3D shape analysis of the supraspinatus muscle: a clinical study of the relationship between shape and pathology," *Academic Radiology*, vol. 14, no. 10, pp. 1229–1241, 2007.
- [16] S. Y. Kim, E. L. Boynton, K. Ravichandiran, L. Y. Fung, R. Bleakney, and A. M. Agur, "Three-dimensional study of the musculotendinous architecture of supraspinatus and its functional correlations," *Clinical Anatomy*, vol. 20, no. 6, pp. 648–655, 2007.
- [17] S. M. Thompson, P. Reilly, R. J. Emery, and A. M. J. Bull, "An anatomical description of the pennation angles and central tendon angle of the supraspinatus both in its normal configuration and with full thickness tears," *Journal of Shoulder and Elbow Surgery*, vol. 20, no. 6, pp. 899–903, 2011.
- [18] V. Karas, V. M. Wang, A. Dhawan, and B. J. Cole, "Biomechanical factors in rotator cuff pathology," *Sports Medicine and Arthroscopy Review*, vol. 19, no. 3, pp. 202–206, 2011.
- [19] S. Kim, R. Bleakney, E. Boynton et al., "Investigation of the static and dynamic musculotendinous architecture of supraspinatus," *Clinical Anatomy*, vol. 23, no. 1, pp. 48–55, 2010.
- [20] S. Y. Kim, D. D. Lunn, R. J. Dyck, L. J. Kirkpatrick, and B. W. C. Rosser, "Fiber type composition of the architecturally distinct regions of human supraspinatus muscle: a cadaveric study," *Histology and Histopathology*, vol. 28, no. 8, pp. 1021–1028, 2013.
- [21] J. A. Hermenegildo, S. L. Roberts, and S. Y. Kim, "Innervation pattern of the suprascapular nerve within supraspinatus: a three-dimensional computer modeling study," *Clinical Anatomy*, vol. 27, no. 4, pp. 622–630, 2014.
- [22] P. L. Powell, R. R. Roy, P. Kanim, M. A. Bello, and V. R. Edgerton, "Predictability of skeletal muscle tension from architectural determinations in guinea pig hindlimbs," *Journal of Applied Physiology*, vol. 57, no. 6, pp. 1715–1721, 1984.
- [23] D. C. Meyer, K. Wieser, M. Farshad, and C. Gerber, "Retraction of supraspinatus muscle and tendon as predictors of success of rotator cuff repair," *American Journal of Sports Medicine*, vol. 40, no. 10, pp. 2242–2247, 2012.
- [24] S. L. Delp, F. C. Anderson, A. S. Arnold et al., "OpenSim: open-source software to create and analyze dynamic simulations of movement," *IEEE Transactions on Biomedical Engineering*, vol. 54, no. 11, pp. 1940–1950, 2007.
- [25] K. R. Saul, X. Hu, C. M. Goehler et al., "Benchmarking of dynamic simulation predictions in two software platforms using an upper limb musculoskeletal model," *Computer Methods in Biomechanics and Biomedical Engineering*, vol. 18, no. 13, pp. 1445–1458, 2014.
- [26] S. L. Delp, A. S. Arnold, R. A. Speers, and C. A. Moore, "Hamstrings and psoas lengths during normal and crouch gait: implications for muscle-tendon surgery," *Journal of Orthopaedic Research*, vol. 14, no. 1, pp. 144–151, 1996.
- [27] A. G. Hannam, I. K. Stavness, J. E. Lloyd, S. S. Fels, A. J. Miller, and D. A. Curtis, "A comparison of simulated jaw dynamics in models of segmental mandibular resection versus resection with alloplastic reconstruction," *The Journal of Prosthetic Dentistry*, vol. 104, no. 3, pp. 191–198, 2010.
- [28] A. M. Agur, V. Ng-Thow-Hing, K. A. Ball, E. Fiume, and N. H. McKee, "Documentation and three-dimensional modelling of human soleus muscle architecture," *Clinical Anatomy*, vol. 16, no. 4, pp. 285–293, 2003.
- [29] D. Lee, K. Ravichandiran, K. Jackson, E. Fiume, and A. Agur, "Robust estimation of physiological cross-sectional area and geometric reconstruction for human skeletal muscle," *Journal of Biomechanics*, vol. 45, no. 8, pp. 1507–1513, 2012.
- [30] D. Lee, Z. Li, Q. Z. Sohail, K. Jackson, E. Fiume, and A. Agur, "A three-dimensional approach to pennation angle estimation for human skeletal muscle," *Computer Methods in Biomechanics and Biomedical Engineering*, vol. 18, no. 13, pp. 1474–1484, 2015.
- [31] H. Ellman, "Diagnosis and treatment of incomplete rotator cuff tears," *Clinical Orthopaedics and Related Research*, no. 254, pp. 64–74, 1990.
- [32] D. C. Meyer, M. Farshad, N. A. Amacker, C. Gerber, and K. Wieser, "Quantitative analysis of muscle and tendon retraction in chronic rotator cuff tears," *American Journal of Sports Medicine*, vol. 40, no. 3, pp. 606–610, 2012.
- [33] M. A. Zumstein, J. B. Hempel, J. Hodler, and C. Gerber, "The clinical and structural long-term results of open repair of massive tears of the rotator cuff," *The Journal of Bone and Joint Surgery—American Volume*, vol. 90, no. 11, pp. 2423–2431, 2008.
- [34] G. M. Gartsman and J. C. Milne, "Articular surface partial-thickness rotator cuff tears," *Journal of Shoulder and Elbow Surgery*, vol. 4, no. 6, pp. 409–415, 1995.
- [35] C.-Y. Huang, V. M. Wang, R. J. Pawluk et al., "Inhomogeneous mechanical behavior of the human supraspinatus tendon under uniaxial loading," *Journal of Orthopaedic Research*, vol. 23, no. 4, pp. 924–930, 2005.
- [36] R. L. Lieber, *Skeletal Muscle Structure, Function, and Plasticity: The Physiological Basis of Rehabilitation*, Lippincott Williams & Wilkins, Baltimore, Md, USA, 3rd edition, 2010.
- [37] C. L. Mendias, S. M. Roche, J. A. Harning et al., "Reduced muscle fiber force production and disrupted myofibrillar architecture in patients with chronic rotator cuff tears," *Journal of Shoulder and Elbow Surgery*, vol. 24, no. 1, pp. 111–119, 2015.
- [38] C. Gerber, D. C. Meyer, A. G. Schneeberger, H. Hoppeler, and B. von Rechenberg, "Effect of tendon release and delayed repair on the structure of the muscles of the rotator cuff: an experimental study in sheep," *The Journal of Bone & Joint Surgery—American Volume*, vol. 86, no. 9, pp. 1973–1982, 2004.
- [39] J. N. Gladstone, J. Y. Bishop, I. K. Y. Lo, and E. L. Flatow, "Fatty infiltration and atrophy of the rotator cuff do not improve after

rotator cuff repair and correlate with poor functional outcome,” *The American Journal of Sports Medicine*, vol. 35, no. 5, pp. 719–728, 2007.

- [40] M. E. Hantes, G. K. Karidakis, M. Vlychou, S. Varitimidis, Z. Dailiana, and K. N. Malizos, “A comparison of early versus delayed repair of traumatic rotator cuff tears,” *Knee Surgery, Sports Traumatology, Arthroscopy*, vol. 19, no. 10, pp. 1766–1770, 2011.